On the Area of Feasible Solutions for rank-deficient problems: II. The geometric construction

Mathias Sawall[a], Tomass Andersons[a], Klaus Neymeyr[a,b]

[a] *Universität Rostock, Institut für Mathematik, Ulmenstrasse 69, 18057 Rostock, Germany*
[b] *Leibniz-Institut für Katalyse, Albert-Einstein-Strasse 29a, 18059 Rostock*

Abstract

A multivariate curve resolution problem is said to suffer from a rank-deficiency if the rank of the spectral data matrix is less than the number of the involved chemical species. A rank-deficiency is caused by linearly dependent (in the sense of linear algebra) concentration profiles or spectra of the pure components. The rank-loss is propagated to the spectral mixture data according to the bilinear Lambert-Beer superposition.
This work deals with factor ambiguities for rank-deficient problems and presents an approach for the geometric construction of the area of feasible solutions (AFS). The focus is on the case that the rank-deficient matrix factor has the rank three and the number of chemical species equals at least four. The AFS construction works with polygons tightly enclosing the inner polygon, namely with quadrangles in the case of four chemical species, pentagons for five species and so on.

Key words: multivariate curve resolution, area of feasible solutions, rank-deficiency, Borgen plots.

1. Introduction

If a (time) sequence of spectra taken from spectral measurements, e.g., by observation of a chemical reaction system, is stored in a matrix, then the spectral recovery problem consists of the reconstruction of the pure component profiles. For so-called *rank-regular* or *full-rank* problems the pure profiles are reconstructable by linear combinations of the row vectors respectively column vectors of the spectral data matrix. For *rank-deficient* problems the rank of the spectral data matrix is smaller than the number of chemical species and the spectral recovery problem is more difficult.

A fundamental problem of calculating the true pure component profiles is the lack of their uniqueness even if high-dimensional spectral data is available for both rank-regular (full-rank) and rank-deficient problems. Three approaches to ambiguity analyses are known for rank-regular problems. A first approach is the enclosure of the feasible bands by band boundaries [27, 11]. A second approach is the systematic analysis of the factor ambiguity by means of the area of feasible solutions (AFS, [3, 7, 26]). Third, a sensor-wise estimation can be used to determine the boundaries of the feasible profiles [16]. The AFS is a low-dimensional representation of all feasible pure profiles in terms of the expansion coefficients with respect to the bases of left and right singular vectors of the spectral data matrix. The AFS supports a systematic analysis of the factor ambiguity. For rank-regular problems several methods are known for a numerical computation of the AFS. On the one hand, these are geometric construction algorithms and on the other hand, genuinely numerical approximation methods [26, 7]. The well-known geometric construction, which leads to the so-called Borgen or Borgen-Rajko plots, is restricted to spectral data taken from chemical systems with only three species. The construction works with tight triangles located between the boundary curves of the outer polygon and the inner polygon in the U- and the V-space [3, 19, 12, 2].

The recent work [25] suggests a generalized AFS construction for rank-deficient problems in combination with a *numerical* algorithm for practical AFS computations. The algorithm uses inflating polygons, similar to [24], but with some modifications concerning the dual factor. Here, we introduce a *geometric construction* of the rank-deficient AFS by extending the geometric construction as known from the rank-regular case. The extended method works for spectral data matrices of the rank three, but the number of absorbing species equals four, five or is even larger. The generalized method works with polygons instead of triangles. The vertices of these polygons represent the complete factors in the U- respectively the V-space. For example, quadrangles are used for four-component systems, pentagons serve to represent pure component factors for five-component systems and so on. These polygons enclose the inner polygon. Tightly enclosing polygons serve to construct the so-called inner boundary curve of the AFS; see [2] for the definition of the inner boundary curve and [3, 19] for the construction of this curve. Depending on the number

of species either a tangent rotates around the inner polygon (odd number of components) or a vertex moves along the boundary of the outer polygon to compute a discretization of the inner boundary curve of the AFS.

The presented theory of this paper applies to chemical systems with at least four chemical species. We discuss an example problem with four species and with the rank 3. For mathematical reasons a system with only three chemical species including a rank-deficiency so that the spectral data matrix has the rank 2 cannot be considered. The decisive fact is that any nonnegative rank-2 matrix always has a non-negative factorization, see [28, 4]. Therefore, no rank-deficiency in the sense of a missing nonnegative factorization with matrices of the same rank can be stated and no generalized AFS can be defined and calculated. However, in such cases a "standard" AFS can be computed, but then at least one of the true profiles is not represented by the AFS or, in other words, at least all feasible profiles of a certain pure component would have no chemical meaning or interpretation.

1.1. Organization of the paper

Section 2 introduces the low-dimensional abstract space representation of the multivariate curve resolution (MCR) problem for rank-deficient problems. The key ingredients are rotating polygons with a minimal number of vertices. Some crucial concepts from [25] are rehashed and important variables are introduced. Then Sec. 3 presents the new construction algorithms which are based on a point orbiting on the boundary of the outer polygon and using a tangent rotating around the inner polygon. Sec. 4 demonstrates how to use the geometric construction for noisy data. Further, we highlight differences to the numerical computation approach from [25].

2. Geometric AFS constructions for rank-deficient problems

This section introduces the new geometric construction of the generalized AFS for rank-deficient MCR problems. See [3, 14, 19, 8, 12, 26] and others for more details on the general approach of reconstructing the pure component profiles by using a truncated singular value decomposition (SVD). We assume in this and the next section that the rank-deficiency is caused by the spectral factor for which we use the variable S, cf. [25]. This assumption does not restrict the generality of the approach since a transposition of the spectral data matrix swaps the concentration factor with the spectral factor. The assumption that the rank-deficiency of the spectral data matrix D is caused by the spectral factor implies that each column of S, namely the pure component spectra, are representable with respect to the first $s = \operatorname{rank}(D)$ right singular vectors of D.

2.1. Preliminary considerations and important variables

Let $U\Sigma V^{\mathrm{T}}$ be a truncated SVD of the given k-by-n spectral data matrix D. Then all components of the first left singular vector $U(:,1)$ and the first right singular vector $V(:,1)$ have the same sign, namely they are either positive or negative. This is guaranteed (under the weak assumption of the so-called irreducibility of D) by the Perron-Frobenius theorem. See [22, 15] for the MCR-related background. Without loss of generality we can even assume a componentwise positivity of $U(:,1)$ and $V(:,1)$; otherwise U and V are substituted by $-U$ and $-V$ which again form an SVD.

The decisive geometric objects for the AFS construction in the V-space, namely the space of spectral profiles, are the outer polytope $\mathcal{F}$ and the inner polytope $\mathcal{I}$

$$\begin{aligned}\mathcal{F} &= \left\{x \in \mathbb{R}^{s-1} : \ (1, x^{\mathrm{T}})V^{\mathrm{T}} \geq 0\right\},\\ \mathcal{I} &= \operatorname{convhull}(\{a_1, \ldots, a_k\})\end{aligned}$$

with the *data representing points* $a_i \in \mathbb{R}^{s-1}$ being defined as

$$a_i = \frac{(U\Sigma)^{\mathrm{T}}(2:s, i)}{(U\Sigma)^{\mathrm{T}}(1, i)}, \quad i = 1, \ldots, k. \tag{1}$$

Later, we restrict the analysis to $s = 3$. Then the polytopes for $s - 1 = 2$ dimensions are simply polygons.

The nonnegative rank is an important property of a matrix in a rank-deficient problem. The nonnegative rank $m := \operatorname{rank}_+(D)$ of a nonnegative matrix $D \in \mathbb{R}^{k\times n}$ is defined to be the smallest number $m \in \mathbb{N}$ so that nonnegative matrices $C \in \mathbb{R}^{k\times m}$ and $S \in \mathbb{R}^{m\times n}$ exist which represent a nonnegative factorization $D = CS^{\mathrm{T}}$ of the spectral data matrix, see [9, 4, 6]. Let $m = \operatorname{rank}_+(D)$ be the number of anticipated chemical components and let $s = \operatorname{rank}(D)$ be the rank of D. Necessarily, it holds that $s \leq m$. As mentioned above, we assume the factor S to carry the rank-deficiency. Therefore S can be reconstructed columnwise in terms of linear expansions of the first s right singular vectors. Similarly to [25],

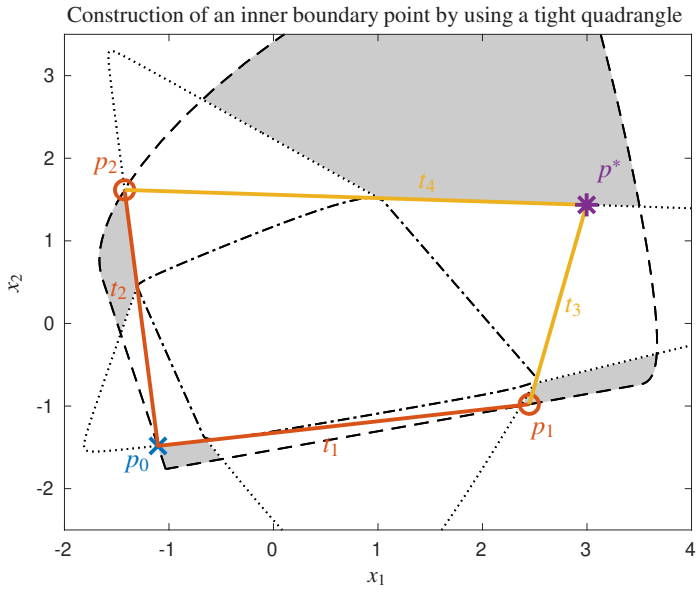

Figure 1: This figure illustrates the construction of an inner boundary point of the AFS of a rank-deficient matrix with rank 3 and nonnegative rank 4. Hence quadrangles in $\mathcal{F}$ are to be constructed which enclose $\mathcal{I}$. The boundary of the outer polygon is plotted as a black dashed line and the boundary of the inner polygon is drawn by a black dash-dotted line. These two polygons are determined by the given model matrix. The starting point for the construction of the quadrangle is a first vertex p_0 on the boundary of the outer polygon (blue cross). Then the two tangents to the inner polygon which also run through p_0 are t_1 and t_2 (red lines). Their points of intersection with the outer polygon (aside from the given point p_0) are p_1 and p_2 (red circles). Starting from p_1 and p_2 the next two tangents to $\mathcal{I}$ are t_3 and t_4 (ochre). Their point of intersection p^* is contained in $\mathcal{F}$ (if this is not the case, then no feasible factorization is possible starting from p_0) and is a point on the inner boundary curve of the AFS (purple star). By repeating this construction with other initial points, we can construct the complete inner boundary curve of the AFS. The result is the black dotted curve, where we have also plotted parts of the curve outside $\mathcal{F}$. The generalized AFS are all regions in $\mathcal{F}$ that lie between the dotted curve and the boundary curve of $\mathcal{F}$. These regions are marked as gray areas. The model data matrix underlying this illustration is taken from Sec. 6 of [25] and all steps apply to the factor C.

a transformation by $T \in \mathbb{R}^{m\times s}$ serves to form the m pure component profiles in terms of the first s singular vectors with

$$T = \begin{pmatrix} 1 & x \\ \mathbf{1} & W \end{pmatrix} \tag{2}$$

where $\mathbf{1} = (1, \ldots, 1)^T \in \mathbb{R}^{m-1}$ as well as $W \in \mathbb{R}^{(m-1)\times(s-1)}$. Then the generalized AFS for rank-deficient data D reads

$$\begin{aligned} \mathcal{N} = \Big\{ x \in \mathbb{R}^{s-1} :\ & \text{exists } C \in \mathbb{R}_+^{k\times m} \text{ and } T \in \mathbb{R}^{m\times s} \\ & \text{with } T(1,:) = (1, x^{\mathrm{T}}),\ TV^{\mathrm{T}} \geq 0 \\ & \text{and } D = CTV^{\mathrm{T}} \Big\}. \end{aligned}$$

2.2. Low-dimensional representation for rank-deficient problems by polygons instead of simplices

For the rank-regular (full-rank) case the vertices of a simplex nested between the inner and the outer polytope represent a complete nonnegative factorization of D. However, for a rank-deficient matrix under the given assumptions there does not exist a simplex located in the outer polytope which encloses the inner polytope. The latter statement is justified as follows. For a rank-deficient matrix it holds that $s = \operatorname{rank}(D) < \operatorname{rank}_+(D) = m$, and the nonnegative rank m is the minimal number so that a polytope $\mathcal{P}$ in the $(s-1)$-dimensional space with m vertices exists that is located in $\mathcal{F}$ and includes $\mathcal{I}$, see for instance [1, 29, 6]. This is the reason why a polytope with exactly m vertices is required. Then the geometric enclosure relations are equivalent to the existence of a factorization of the spectral data matrix with nonnegative matrix factors C and S^{T}. In more detail the relations are as follows. The data points a_i by (1) are convex combinations of the vertices of the polytope $\mathcal{P}$ being located in $\mathcal{F}$ if and only if $\mathcal{P}$ encloses the inner polytope [20]. Hence the polytope $\mathcal{P}$ results in a factor S which can be extended by an associated factor C to one feasible MCR-solution. In the remainder of this work we only consider the geometric construction for the case $\operatorname{rank}(D) = s = 3$. Therefore we consider only geometric constructions in the $(s-1=2)$-dimensional space. This means that we consider enclosing quadrangles, pentagons or polygons with more vertices in the two-dimensional plane.

3. The geometric AFS construction algorithm for the rank-deficient case

In analogy to the rank-regular (full-rank) case, the goal of the algorithm is to determine the inner boundary curve of the AFS. The remaining part of the boundary of the AFS belongs to the boundary of the outer polygon and is easy to determine by the nonnegativity constraints. In the following we introduce two variants of the construction algorithm. In each case tight polygons are computed with all edges touching (but not intersecting) the inner polygon and with all but one vertices being located on the boundary of the outer polygon. Depending on whether $m = \mathrm{rank}_+(D)$ is even or not, a point on the outer polygon (for simplicity, we refer to a 2D polygon by its boundary curve) or a tangent to the inner polygon is the starting point for the construction. The remaining vertex is on the inner boundary curve. The point orbits on the boundary of the outer polygon for even m, respectively the tangent rotates around the inner polygon for odd m. In both cases a smallest possible polygon is searched for which includes the given vertex or (part of the) tangent and encloses the inner polygon. Next we explain the case $m = 4$ in detail and then give some remarks on more general cases.

3.1. Geometric AFS constructions by quadrangles

This section introduces the geometric construction for the case $\mathrm{rank}_+(D) = 4$. The goal is to construct quadrangles with three vertices on the boundary of the outer polygon and with all four edges being tangents of the inner polygon. By definition a tangent of a polygon is a line touching the polygon in a way that the entire polygon lies on one side of the line. This definition includes that the tangent is uniquely determined on all boundary points that are not vertices and that there is a range of possible tangents in any vertex of the polygon. By studying the geometric relations of such constrained tight polygon enclosures one is led to the following statements. In order to have analogous point-tangent constructions and an equal number of tangents on both sides of the inner polygon, the construction of a quadrangle starts with a vertex on the edge of the outer polygon. In order to compute the complete inner boundary curve many quadrangles are to be constructed and one point of intersection of the initial tangent rotates around the boundary of the outer polygon.

Let $p_0 \in \mathbb{R}^2$ be a certain point being located on the numerical representation, or discretization, of the boundary of $\mathcal{F}$. The construction of a quadrangle is as follows:

1. Construct two non-identical tangents t_1 and t_2 to the inner polygon which both run through p_0.
2. Compute the two additional points of intersection p_1 and p_2 of t_1 and t_2 with the boundary of the outer polygon.
3. Compute for p_1 and p_2 the two additional tangents t_3 and t_4 to the inner polygon being different to t_1 and t_2 so that t_3 runs through p_1, namely $p_1 \in t_3$, as well as that t_4 runs through p_2, that is $p_2 \in t_4$.
4. Compute the point of intersection p^* of t_3 and t_4. Then p^* is a point on the inner boundary curve of the generalized AFS and is of interest for the AFS construction if it is contained in the outer polygon.

Fig. 1 illustrates the construction for one quadrangle in application to model data as introduced in Sec. 6 of [25]. It is worth noting that the construction applies to the factor C carrying the rank-deficiency for this model problem. The next theorem provides a geometric argumentation that the constructed point p^* lies on the inner boundary curve of the generalized AFS if $p^* \in \mathcal{F}$.

Theorem 3.1. *For $s = 3$ and $m = 4$ it is not possible to move the constructed point p^* in the direction of the origin, namely the point $(0, 0)$, without violating at least one condition associated with the non-negativity constraints of all remaining profiles.*

Hence, p^* is a point on the inner boundary curve of the AFS. Further, p^* is a feasible point if and only if $p^* \in \mathcal{F}$.

Proof. Due to the construction all tangents touch the inner polygon and at least all but one vertices of the quadrangle are on the boundary of the outer polygon. Moving p^* on a straight line towards the origin would open the cone between these two tangents because they cannot cross the interior of $\mathcal{I}$. Then the points of intersection with the first two tangents would leave the outer polygon which breaks the nonnegativity constraints for the represented profiles. On the other hand p_0 cannot be moved outside on a straight line through p_0 and the origin without leaving $\mathcal{F}$. So p_1 and p_2 cannot simultaneously be moved closer to p^* on the boundary curve of of $\mathcal{F}$. The same property holds for any other point p_0 due to the convexity of $\mathcal{F}$.

Finally, if and only if p^* is contained in the outer polygon together with all other vertices, then the construction of the quadrangle enclosing the inner polygon guarantees the nonnegativity of both factors of the spectral data matrix D, cf. [20]. □

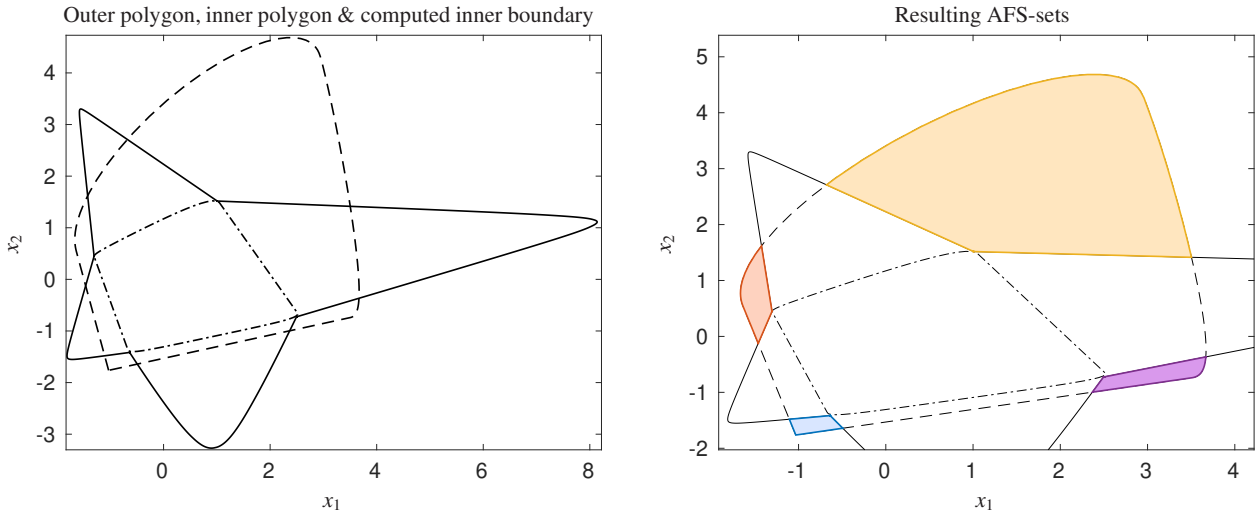

Figure 2: The generalized AFS for the Michaelis-Menten problem computed by geometric construction, see Sec. 3.2 and Sec. 6 of [25]. Left: The outer polygon is plotted by a dashed line, the inner polygon by a dash-dotted line and the inner boundary curve by a solid line. The boundary curve discretization is based on nearly 5000 points. Right: The final four AFS subsets are shown as colored sets. These regions are located between the inner boundary curve in the interior of $\mathcal{F}$ and the boundary curve of $\mathcal{F}$. The associated pure component profiles and the bands of feasible profiles are shown in Fig. 3.

For any starting point p_0 the quadrangle construction results in a final point p^* whose feasibility can easily be checked by computing the associated profile and then by testing its nonnegativity. By circulating p_0 along the boundary of the outer polygon and by regularly repeating numerical quadrangle constructions a discrete point curve is constructed. Points which are not in $\mathcal{F}$ can be ignored. The points of interest in $\mathcal{F}$ form a discretization of the inner boundary curve of the generalized AFS. The discrete circulation of p_0 should follow some rules. For instance, all vertices of $\mathcal{F}$ should be considered as starting points for the quadrangle construction as they seem to be potentially crucial for an accurate representation of the inner boundary curve. Further, each facet of $\mathcal{F}$ should be discretized in a proper way so that it is covered by equidistant starting points p_0. In order to guarantee a sufficiently fine resolution of the inner boundary curve, the algorithm requires a correspondingly large number of starting points on the boundary of $\mathcal{F}$. If the generalized AFS includes single point subsets (or very small AFS subsets), then sometimes a very fine discretization of the curve of starting points cannot be sufficient. Therefore each edge of the inner polygon $\mathcal{I}$ should be involved in at least one quadrangle construction. Fig. 2 illustrates a complete discretization of the inner boundary curve (including parts which leave $\mathcal{F}$ and which are therefore meaningless for the generalized AFS construction) for the model problem from Sec. 6 of [25], see also the following Sec. 3.2. Figure 3 shows the bands of feasible concentration profiles which are associated with the four colored regions of the AFS. Finally, we note that in rare cases sections of the inner boundary curve can only be correctly determined for a locally very dense sequence of starting points.

3.2. Michaelis-Menten model problem

We reuse, see [25], for numerical experiments the Michaelis-Menten kinetic

$$S + K \underset{\kappa_{-1}}{\overset{\kappa_1}{\rightleftharpoons}} [K\text{-}S] \xrightarrow{\kappa_2} P + K$$

as a simple rank-deficient reaction system. The kinetic parameters are taken as $\kappa_1 = 30$, $\kappa_{-1} = 0.1$ and $\kappa_2 = 3$ and the initial concentrations are $c_S(0) = 1$, $c_K(0) = 0.1$ and $c_{[K\text{-}S]}(0) = c_P(0) = 0$. The resulting AFS is shown in Figs. 2. The pure component profiles are plotted in Fig. 3. The substrate S and the catalyst K first form the catalyst-substrate complex $[K\text{-}S]$ which then decays to the product P plus K. For this reaction system with four chemical species two mass-balance equations hold for the time-dependent concentration values

$$c_S(t) + c_{[K\text{-}S]}(t) + c_P(t) = c_S(0) + c_{[K\text{-}S]}(0) + c_P(0) = 1 \quad \text{and} \quad c_K(t) + c_{[K\text{-}S]}(t) = c_K(0) + c_{[K\text{-}S]}(0) = 0.1.$$

The right-hand sides of these equations are constants that are given by the the initial concentration values. These two *affine-linear* combinations can be reformulated as a single linear dependence equation between the concentration value functions (in the sense of linear algebra that a linear combination with at least one non-zero coefficient can

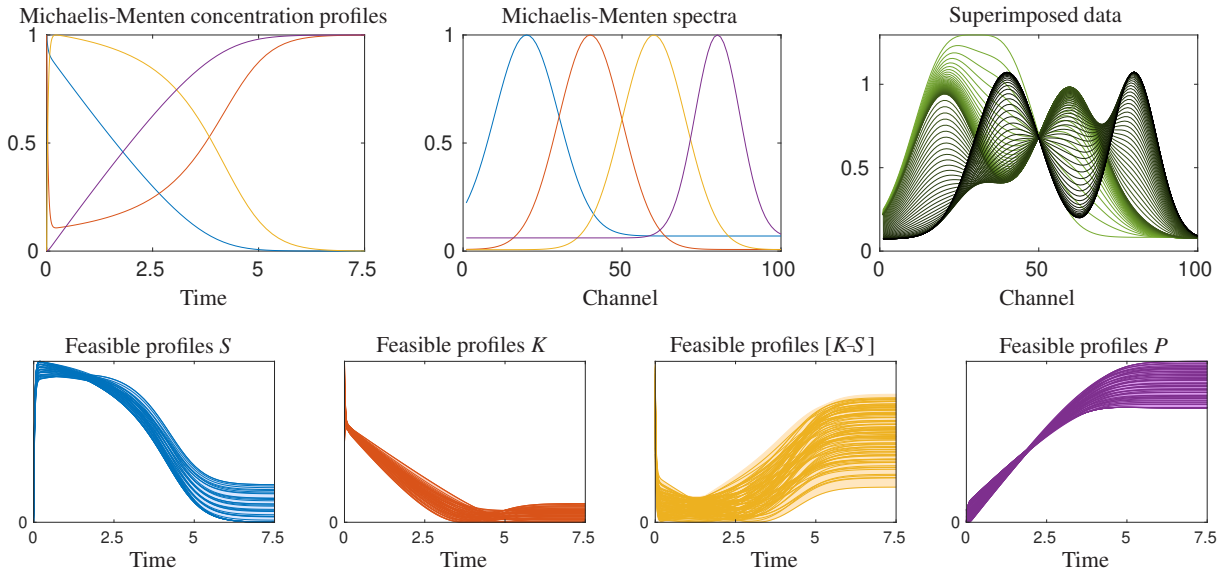

Figure 3: Upper row of plots: The concentration profiles and spectra, all profiles are normalized with maximum equal to 1, of the four species of the Michaelis-Menten model from Section 3.2 are shown together with the resulting superimposed mixture data. The color gradient of the mixture spectra turns from green (at $t_1 = 0$) to black (at $t_{\text{end}} = 7.5$). These data are used for the generation of Fig. 2. See Sec. 3.2 for details on the data. Lower row of plots: Based on the generalized AFS from Fig. 2, the sets of feasible concentration profiles are computed for each subset of the AFS $\mathcal{N}$.

represent the null function). In other words, a nonzero vector z exists so that $Cz = 0$. Thus C has only the rank 3 (instead of 4).

The generalized AFS is computed with parameters $m = 4$ and $s = 3$ for this model data set. The results are shown in Fig. 2. The AFS consists of four isolated subsets. Each subset is associated with a band of feasible profiles. To compute these bands, each subset is covered with a relatively fine mesh with more or less uniformly distributed nodes. Then for each node point x the associated profile $c = U\Sigma(1, x^{\mathrm{T}})^{\mathrm{T}}$ is computed. The four plots of all these feasible profiles are shown in the lower row of Fig. 3.

3.3. Geometric construction for even m larger than 4

The proposed algorithm for quadrangles can be extended to problems with a larger nonnegative rank m. If m is an even number, then the symmetric construction remains analogous to that in Sec. 3.1, but uses more tangents in order to enclose the inner polygon. The number of edges of the polygons being enclosed from the outside and inside equals m. All edges of these polygons are tangents of $\mathcal{I}$ and all but one of its vertices are located on the boundary of $\mathcal{F}$.

3.4. Geometric construction for odd m larger than 4

For an odd nonnegative rank m, we explain the procedure for $m = \operatorname{rank}_+(D) = 5$, namely for pentagon constructions. For $m = 7, 9, \ldots$ the idea remains the same. For tight pentagon constructions we use again point-tangent constructions with an equal number of tangents on both sides of the inner polygon. The construction starts with a tangent. To obtain the inner boundary curve of the generalized AFS, a tangent line rotates in a discretized manner around the inner polygon. The construction principles coincide with the classical Borgen plot for $\operatorname{rank}_+(D) = \operatorname{rank}(D) = 3$, which uses rotating triangles.

Let t_0 be a tangent of the inner polygon. Then the procedure is as follows:

1. Compute the points of intersection p_1 and p_2 of t_0 with the outer polygon and get the first two vertices.
2. Compute the next two edges t_1 and t_2 as tangents to the inner polygon with $p_1 \in t_1$ and $p_2 \in t_2$ as well as $t_1 \neq t_0$ and $t_2 \neq t_0$.
3. Compute the two new points of intersection p_3 and p_4 of t_1 and t_2 with the outer polygon. Finally, determine the two tangents t_3 and t_4 running through p_3 respectively p_4 so that $t_3 \neq t_1$ and $t_4 \neq t_2$.
4. If the point of intersection p^* of t_3 and t_4 is located in $\mathcal{F}$, then it is an inner boundary point of the generalized AFS.

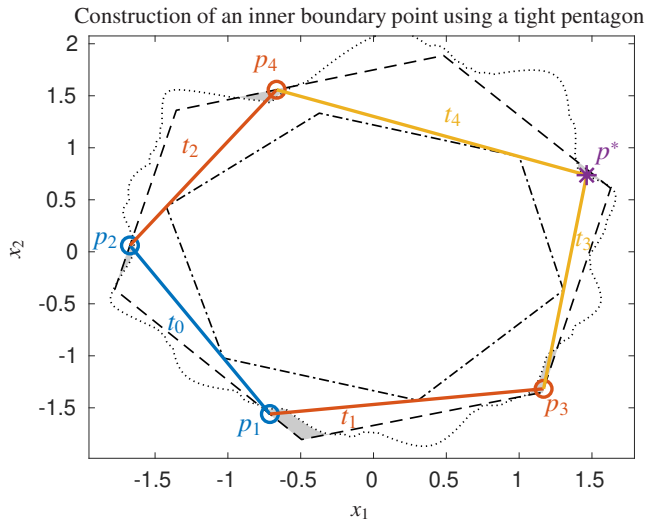

Figure 4: Construction of an inner boundary point using a pentagon in application to a model problem with $\mathrm{rank}(D) = 3$ and $\mathrm{rank}_+(D) = 5$. The outer polygon (black dashed line) and the inner polygon (black dash-dotted line) are fixed. The construction of the pentagon starts with the tangent t_0 (blue) of the inner polygon. Its points of intersection with the boundary of the outer polygon are p_1 and p_2 (blue), and the next two tangents are t_1 and t_2 (red). Ths step is repeated and leads to the two tangents t_3, t_4 (ochre). Their point of intersection p^* is a point on the inner boundary curve (purple star). The complete inner boundary curve is the dotted black line. The geometric area of the resulting generalized AFS is small. The AFS consists of five isolated subsets marked in gray. These subsets of the AFS are located between the inner boundary curve and the boundary of the outer polygon.

The starting edge t_0 rotates around the inner polygon. As explained in the first paragraph of Sec. 3.1 any vertex of the inner polygon has a range of possible tangents. This process results in a discretization of the inner boundary curve. Fig. 4 explains the construction for a tight pentagon around the inner polygon for a 6×6 model data matrix. The resulting inner boundary curve of the generalized AFS resulting from all pentagon constructions is the dotted line.

4. Noise handling and how the geometric construction differs from a genuinely numerical approximation

4.1. The geometric construction for noisy data

The presented algorithm works with the two fixed polygons $\mathcal{F}$ and $\mathcal{I}$. For noisy data several aspects are to be considered. Firstly, noise tends to break rank-deficiencies. This phenomenon is comparable to the fact that a singular matrix to which noise is added turns almost always into a regular matrix (which, however, is poorly conditioned). Thus one can expect for noisy data that $\mathrm{rank}(D) = \mathrm{rank}_+(D) = \min(k, n)$. Hence, the values s and m must be selected manually with careful consideration of the noise level in order to calculate meaningful results. Secondly, if the nonnegativity restrictions are applied in a strict sense, then the computations for the polygons $\mathcal{F}$ and $\mathcal{I}$ can result in empty AFS-sets. In particular, vertices of $\mathcal{I}$ can leave the outer polygon $\mathcal{F}$ (then the data contains negative entries, e.g., after background subtraction), the set $\mathcal{F}$ does not include the origin or even $\mathcal{F}$ can be an empty set. However, there are ways how to compute an approximation of the inner and the outer polygon for noisy data so that these polygons are close to the respective polygons for noise-free data.

A way how to approximate the inner and the outer polygon for noisy or perturbed data for the case $\mathrm{rank}(D) = 3$ is explained in [23]. The idea is to start with the computation of an approximation of the two outer polygons $\mathcal{F}_S$ and $\mathcal{F}_C$ by means of the inverse polygon inflation algorithm [24] with a weakened nonnegativity constraint, namely negative entries of small magnitude are accepted in the profiles. By using duality techniques [10, 18, 21] it is possible to compute approximations of the two dual inner polygons $\mathcal{I}_C$ and $\mathcal{I}_S$. This approach is less sensitive to noise. The resulting polygon approximations are the basis for a subsequent geometric AFS construction. The resulting generalized AFS allows relatively small negative entries in the spectra and concentration profiles.

4.2. Differences to numerical methods

The concept of a generalized AFS is introduced for rank-deficient problems in [25]. There is also a genuinely numerical approximation method for $s = 3$. The algorithm inflates polygons in order to approximate the AFS-subsets. The algorithm works with an adaptive approximation scheme including a local error estimation and includes several

control parameters. The decision whether a point is feasible or not is based on the reconstruction $S^{\mathrm{T}} = TV^{\mathrm{T}}$ and works with a nonnegative least squares (NNLS) algorithm from [13] to check whether a nonnegative C exists so that $D = CS^{\mathrm{T}}$. The geometric algorithm suggested in this work is completely based on the low-dimensional geometric representation in the abstract U and V spaces. The test whether a nonnegative C exists or not is done by checking whether the constructed polygon encloses the inner polygon or not, see also [20]. For noisy data the geometric construction approach works better than the numerical approximation from [25]. The difference is that the NNLS-solver does not allow slightly negative entries. Thus deviations from the non-negativity constraints can only be applied via the outer polygon. In contrast to this the geometric construction works directly with the inner and the outer polygon. As duality allows to compute the inner polygon even for noisy data this approach is more flexible.

The suggested geometric construction for rank-deficient problems is faster than the numerical method from [25] for two reasons. On the one hand, the geometric construction of a tight quadrangle is a simple and direct step which is easy to understand compared to the optimization procedure used in the polygon inflation algorithm where for a given row of T all the remaining rows of this matrix are to be determined by numerical optimization. On the other hand, the decision whether an associated nonnegative factor C exists for a certain polygon is immediately answered by the geometric construction since the constructed polygon includes the inner polygon. This is much faster than applying an NNLS solver in each step of the numerical algorithm. Furthermore, the NNLS solver must be called once for each individual objective function evaluation in each individual optimization step.

5. Summary and conclusion

The geometric construction of the generalized AFS for rank-deficient matrices is an exact and effective procedure. Originally, the geometric AFS construction was developed by Borgen and Kowalski as a tool to analyze the factor ambiguity of MCR solutions for model data. Over the years, the elegant approach has been extended for an applicability to noisy data. Unfortunately, the geometric construction of the inner boundary of the generalized AFS has (until now) been restricted to spectral data matrices with the maximal rank three due to the complexity of the geometric constructions. In principle, the necessary low-dimensional simplex constructions appear to be possible for any $s \geq 2$. The algorithmic hurdles for a construction of the inner boundary spheres for $s > 3$ (instead of the inner boundary curve) still have to be overcome. Such problems are hard to solve since [29] points out that the NMF problem is NP-hard for $s \geq 4$.

The extension of the geometric construction to rank-deficient problems is in some sense straightforward. Nevertheless, the algorithm as presented in this work only returns a discretization of the inner boundary curve similar to the approach in [12]. Here, we do not present a purely analytical approach with a functional representation of the boundary curves as presented in [3, 19, 2] for rank-regular (full-rank) problems. A main advantage of the proposed algorithm is its low effort. The inner and outer polygons are typically easily handable and can be computed for model data as well as for noisy data. Duality relations support the numerical algorithms and improve the stability of the computation of the inner polygon even for noisy data. The geometric construction is not limited by the number of chemical species, but by the number of linearly independent profiles which must equal three. In contrast to rank-regular problems, the generalized AFS is only defined for one factor, namely the factor which carries the rank-deficiency. The other, dual factor needs more information than contained in the first s singular vectors.

The new generalized AFS concept for rank-deficient problems augments the arsenal of techniques such as Borgen-Rajko-plots, grid search or polygon inflation for rank regular problems as well as the profile-based methods MCR-BANDS [5, 27] and N-BANDS [17, 16]. All these methods serve to analyze and to determine the factor ambiguity of MCR-problems.

References

[1] A. Aggarwal, H. Booth, J. O'Rourke, S. Suri, and C. K. Yap. Finding minimal convex nested polygons. *Inf. Comput.*, 83(1):98–110, 1989.

[2] T. Andersons, M. Sawall, and K. Neymeyr. Analytical enclosure of the set of solutions of the three-species multivariate curve resolution problem. *J. Math. Chem.*, 60:1750–1780, 2022.

[3] O.S. Borgen and B.R. Kowalski. An extension of the multivariate component-resolution method to three components. *Anal. Chim. Acta*, 174:1–26, 1985.

[4] J. E. Cohen and U. G. Rothblum. Nonnegative ranks, decompositions, and factorizations of nonnegative matrices. *Linear Algebra Appl.*, 190:149–168, 1993.

[5] P.J. Gemperline. Computation of the range of feasible solutions in self-modeling curve resolution algorithms. *Anal. Chem.*, 71(23):5398–5404, 1999.

[6] N. Gillis and F. Glineur. On the geometric interpretation of the nonnegative rank. *Linear Algebra Appl.*, 437(11):2685 – 2712, 2012.

[7] A. Golshan, H. Abdollahi, S. Beyramysoltan, M. Maeder, K. Neymeyr, R. Rajkó, M. Sawall, and R. Tauler. A review of recent methods for the determination of ranges of feasible solutions resulting from soft modelling analyses of multivariate data. *Anal. Chim. Acta*, 911:1–13, 2016.

[8] A. Golshan, H. Abdollahi, and M. Maeder. Resolution of rotational ambiguity for three-component systems. *Anal. Chem.*, 83(3):836–841, 2011.

[9] D. A. Gregory and N. J. Pullman. Semiring rank: Boolean rank and nonnegative rank factorizations. *J. Combin. Inform. System Sci*, 8(3):223–233, 1983.

[10] R.C. Henry. Duality in multivariate receptor models. *Chemom. Intell. Lab. Syst.*, 77(1-2):59–63, 2005.

[11] J. Jaumot and R. Tauler. MCR-BANDS: A user friendly MATLAB program for the evaluation of rotation ambiguities in multivariate curve resolution. *Chemom. Intell. Lab. Syst.*, 103(2):96–107, 2010.

[12] A. Jürß, M. Sawall, and K. Neymeyr. On generalized Borgen plots. I: From convex to affine combinations and applications to spectral data. *J. Chemom.*, 29(7):420–433, 2015.

[13] C. L. Lawson and R. J. Hanson. *Solving least squares problems*, volume 15 of *Classics Appl. Math.* Society of Industrial and Applied Mathematics, Philadelphia, 1995.

[14] M. Maeder and Y.M. Neuhold. *Practical data analysis in chemistry*. Elsevier, Amsterdam, 2007.

[15] K. Neymeyr and M. Sawall. On the set of solutions of the nonnegative matrix factorization problem. *SIAM J. Matrix Anal. Appl.*, 39:1049–1069, 2018.

[16] A. C. Olivieri. Estimating the boundaries of the feasible profiles in the bilinear decomposition of multi-component data matrices. *Chemom. Intell. Lab. Syst.*, 216:104387, 2021.

[17] A. C. Olivieri and R. Tauler. N-BANDS: A new algorithm for estimating the extension of feasible bands in multivariate curve resolution of multicomponent systems in the presence of noise and rotational ambiguity. *J. Chemom.*, 35(3):e3317, 2021.

[18] R. Rajkó. Natural duality in minimal constrained self modeling curve resolution. *J. Chemom.*, 20(3-4):164–169, 2006.

[19] R. Rajkó and K. István. Analytical solution for determining feasible regions of self-modeling curve resolution (SMCR) method based on computational geometry. *J. Chemom.*, 19(8):448–463, 2005.

[20] M. Sawall, T. Andersons, H. Abdollahi, S. K. Karimvand, B. Hemmateenejad, and K. Neymeyr. Calculation of lower and upper band boundaries for the feasible solutions of rank-deficient multivariate curve resolution problems. *Chemom. Intell. Lab. Syst.*, 226:104577, 2022.

[21] M. Sawall, C. Fischer, D. Heller, and K. Neymeyr. Reduction of the rotational ambiguity of curve resolution techniques under partial knowledge of the factors. Complementarity and coupling theorems. *J. Chemom.*, 26:526–537, 2012.

[22] M. Sawall, C. Kubis, D. Selent, A. Börner, and K. Neymeyr. A fast polygon inflation algorithm to compute the area of feasible solutions for three-component systems. I: Concepts and applications. *J. Chemom.*, 27:106–116, 2013.

[23] M. Sawall, A. Moog, C. Kubis, H. Schröder, D. Selent, R. Franke, A. Brächer, A. Börner, and K. Neymeyr. Simultaneous construction of dual Borgen plots. II: Algorithmic enhancement for applications to noisy spectral data. *J. Chemom.*, 32:e3012, 2018.

[24] M. Sawall and K. Neymeyr. A fast polygon inflation algorithm to compute the area of feasible solutions for three-component systems. II: Theoretical foundation, inverse polygon inflation, and FAC-PACK implementation. *J. Chemom.*, 28:633–644, 2014.

[25] M. Sawall and K. Neymeyr. On the area of feasible solutions for rank-deficient problems: I. Introduction of a generalized concept. *J. Chemom.*, 35(3):e3316, 2020. e3316 cem.3316.

[26] M. Sawall, H. Schröder, D. Meinhardt, and K. Neymeyr. On the ambiguity underlying multivariate curve resolution methods. In S. Brown, R. Tauler, and B. Walczak, editors, *In Comprehensive Chemometrics: Chemcial and Biochemical Data Analysis*, pages 199–231. Elsevier, 2020.

[27] R. Tauler. Calculation of maximum and minimum band boundaries of feasible solutions for species profiles obtained by multivariate curve resolution. *J. Chemom.*, 15(8):627–646, 2001.

[28] L. B. Thomas. Rank factorization of nonnegative matrices (A. Berman). *SIAM Review*, 16(3):393–394, 1974.

[29] S. Vavasis. On the Complexity of Nonnegative Matrix Factorization. *SIAM J. Optim.*, 20(3):1364–1377, 2010.